Synthesis of bis-thiohydantoin derivatives as an antiproliferative agents targeting EGFR inhibitory pathway

Alaa A. Hassan[1] · Ashraf A. Aly[1] · Mohamed Ramadan[2] · Nasr K. Mohamed[1] · Bahaa G. M. Youssif[3] · Hesham A. M. Gomaa[4] · Stefan Bräse[5,6] · Martin Nieger[7] · Amal S. Abd El-Aal[1]

Abstract

(*R*)/(*S*)-the two enantiomers of 3-substituted-1-[2-(5)-3-substituted-4-benzyl-5-oxo-4-phenyl-2-thioxoimid-azolidin-1-yl] ethyl/propyl-5-benzyl-5-phenyl-2-thioxoimidazolidin-4-ones were formed during the diastereoselective reaction between *N*,*N*″-1,ω-alkanediylbis[*N*′-organylthiourea] derivatives and 2,3-diphenylcyclopropenone in refluxing ethanol. The structures of the isolated compounds were confirmed by NMR, IR, mass spectra and elemental analyses. Moreover, single-crystal X-ray structure analysis was also used to elucidate the structure of the isolated compounds. The mechanism describes the reaction was also discussed. The tested compounds showed EGFR inhibitory activity with IC_{50} values ranging from 90 to 178 nM in comparison to the erlotinib as a reference with IC_{50} value of 70 nM. Compound **4c** (R = allyl, n = 3) was found as the most potent antiproliferative, had the highest inhibitory effect on EGFR with an IC_{50} value of 90 nM, compared to erlotinib's IC_{50} value of 70 nM. The second and third-most active compounds were **4e** (R = phenyl, n = 3) and **4d** (R = ethyl, n = 3) and with IC_{50} values of 107 nM and 128 nM. These findings imply that the compounds tested had a significant antiproliferative effect as well as the ability to act as an EGFR inhibitor. Docking studies showed that compound **4c** showed high affinity to EGFR based on its docking score (S; kcal/mol) within five test compounds.

Keywords Thiourea · Cyclopropenone · Thioxoimidazolidin-4-ones · Antiproliferative · EGFR · Heterocycle · Docking

Introduction

Cancer is a serious threat to humans; from a medical standpoint, it is a complicated complex of genetic diseases characterized by abnormal and uncontrolled cell growth and proliferation with the potential to spread throughout the body. Great efforts are currently being made to prevent or reduce cancer incidence and treatment efficacy, but cancer remains a major cause of morbidity and mortality worldwide, and the second leading cause of death in the United States [1–3].

Several natural and synthesized heterocyclic compounds have been investigated as possible pharmacological prodrugs throughout the last few decades [4]. Because of their presence in natural and therapeutically useful chemicals, 2-thiohydantoins (2-thioxo-imidazolidine-4-one), the sulfur analogues of hydantoin, have been recognized as fascinating chemical scaffolds (Fig. 1). Structural modifications of the 2-thiohydantoin ring yield compounds with a diverse range of pharmacological and biological effects, with anticancer activity topping the list [5–9]. The 2-thiohydantoin ring has also been found in the structures of various

✉ Alaa A. Hassan
alaahassan2001@mu.edu.eg

✉ Bahaa G. M. Youssif
bahaa.youssif@pharm.aun.edu.eg; bgyoussif2@gmail.com

1 Chemistry Department, Faculty of Science, Organic Division, Minia University, El-Minia 61519, Minia, Egypt

2 Pharmaceutical Organic Chemistry Department, Faculty of Pharmacy, Al-Azhar University, Assiut Branch, Assiut, Egypt

3 Pharmaceutical Organic Chemistry Department, Faculty of Pharmacy, Assiut University, Assiut 71526, Egypt

4 Department of Pharmacology, College of Pharmacy, Jouf University, Sakaka 72341, Aljouf, Saudi Arabia

5 Institute of Organic Chemistry, Karlsruher Institut Fur Technologie, 76131 Karlsruhe, Germany

6 Institute of Biological and Chemical Systems (IBCS-FMS), Karlsruhe Institute of Technology, 76344 Eggenstein Leopoldshafen, Germany

7 Department of Chemistry, University of Helsinki, A. I. Virtasen Aukio I, P.O. Box 55, 00014 Helsinki, Finland

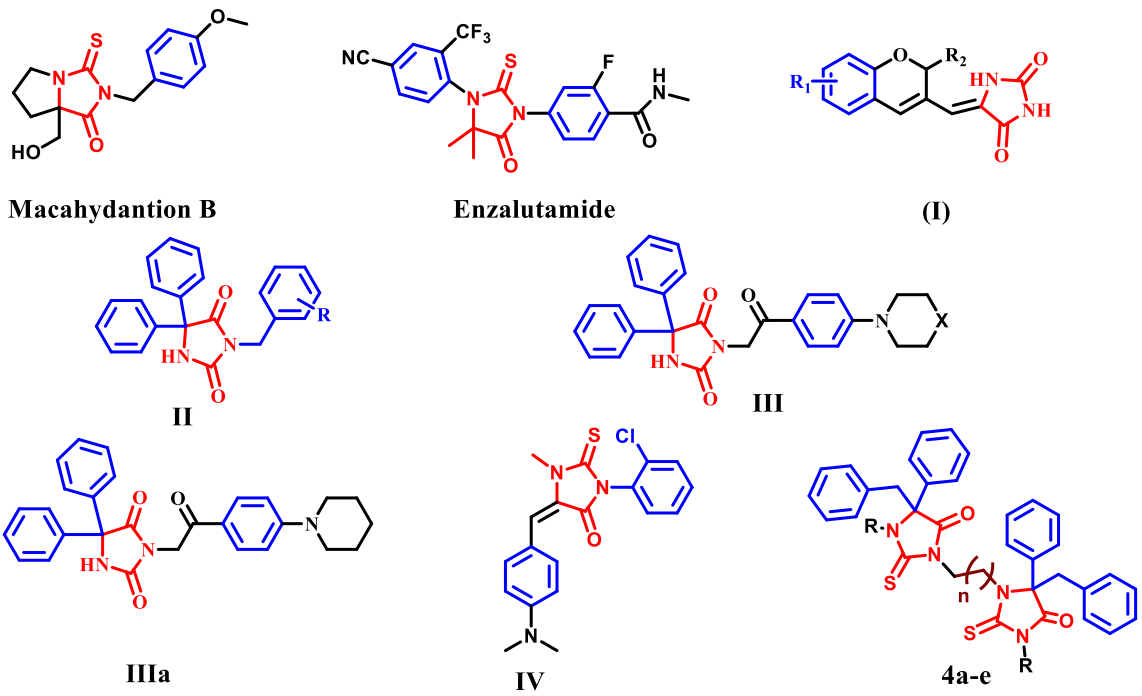

Fig. 1 Structure of hydantoin/thiohydantoin-based derivatives and targets **4a–e**

natural compounds, including Enzalutamide, which has been licensed by the FDA as a treatment for castration-resistant prostate cancer (Fig. 1) [10–12]. Because of the therapeutic importance of hydantoin/2-thiohydantoin-based molecules, the synthesis of a novel class of substituted-hydantoins/2-thiohydantoins has received a lot of interest in the last few decades [13–16].

Aziz Mohammadi et al. described a novel series of hydantoin-chromene hybrids (**I**, Fig. 1) with antiproliferative action [17]. The compounds were tested for antiproliferative efficacy against a panel of five cancer cell lines. In comparison to the reference drug cisplatin, the hydantoin-chromene hybrids demonstrated mild to good anticancer activity. Alanazi et al. developed a series of 3-aminoalkyl/benzyl phenytoins **II** and 3-(4-piperidino/piperazino/morpholino)phenacyl phenytoins **III**, Fig. 1 [18]. These hydantoin derivatives were found to exhibit anticancer action by decreasing epidermal growth factor receptor (EGFR) kinase activity. Interestingly, compound (**IIIa**) shown promising antiproliferative action. Bae et al. identified 3-aryl 5-benzylidene-1-methyl-2-thiohydantoins **IV** as new NADPH-oxidase (NOXs) inhibitors [19]. In that investigation, the synthesised compounds were tested for NOX1 and NOX4 inhibitory activities. **IV** demonstrated good inhibitory action.

Based on the foregoing, we have developed a small set of thiohydantoin-based derivatives **4a–e** (Fig. 1) to be investigated as antiproliferative agents targeting EGFR-TK. In a cell viability assay, the newly developed compounds will be evaluated for their safety profile against normal human cancer cell lines. Further, compounds **4a–e** will be tested against a panel of four human cancer cell lines to determine their IC_{50} values. The most potent compounds will be tested further as EGFR inhibitors. Finally, a molecular docking research will be performed to investigate how these compounds interact with the EGFR active site.

Results and discussion

Chemistry

Scheme 1 depicts the synthetic method for the synthesis of the target compounds **4a–e**. We began our reaction by investigating several aspects. First, different bis[organylthiourea] derivatives **1a–e**, were screened (Scheme 1). Second, the reaction was carried out in different solvents such as absolute ethanol, acetonitrile, toluene, cyclohexane and dimethylformamide (DMF). However, the yields of **4a–e** decrease when using toluene, cyclohexane, acetonitrile and DMF. Finally, by adding excess of the reaction contents, namely diphenylcyclopropenone (**2**) or bithioureas **1a–e**, led to a significant decrease in the yields. There are no reported similar reactions of **2** with the *N*,*N*''-(1,-alkanediyl)bis(*N*'-organylthiourea) derivatives **1a–e**. As a result, the reactions of these groups urge further exploration of the reactivity of **1a–e** toward **2**.

This study was begun by stirring under reflux a solution of *N*,*N*''-(1,*ω*-alkanediyl)bis(*N*'-organyl thiourea)

Scheme 1 Synthesis of compounds **4a–e**

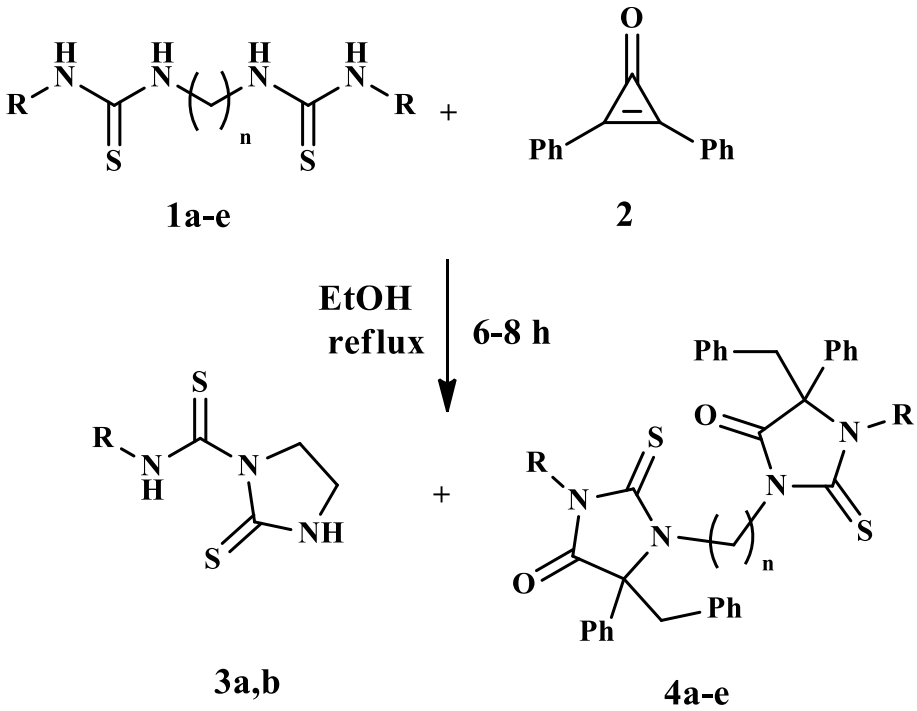

Compound	R	n	Yield of 4 (%)
3a,4a	**Allyl**	**2**	**68**
3b,4b	**Ph**	**2**	**65**
4c	**Allyl**	**3**	**63**
4d	**Et**	**3**	**66**
4e	**Ph**	**3**	**60**

derivatives **1a,b** [20, 21] and 2,3-diphenylcyclopropanone (**2**) in absolute ethanol for 6–8 h. The reaction mixture was concentrated and subjected under chromatographic plates to give 3-substituted-1-(2-(3-substituted-4-benzyl-5-oxo-4-phenyl-2-thioxoimidazolidin-1-yl)ethyl)-5-benzyl-5-phenyl-2-thioxo-imidazolidin-4-ones **4a–e** as the major products (60–68%) and *N*-phenyl-2-thioxo-imidazolidine-1-cashothioamide **3a** and **3b** (4–6%) as a minor products (the structure of **3b** was confirmed by X-ray crystallographic analysis, see SI). Compounds **3a** [22] and **3b** [23] are well-known compounds. Different spectroscopic methods of analysis were used to confirm the structures of compounds **4a–e**. The structures of (thioimidazolidinyl)ethyl-2-thioxoimidazolidinone derivatives **4a–e** showed the stretching frequency range between $\nu = 2980$ and 2960 cm^{-1} due to aliphatic-CH_2, 1680–1664 cm^{-1} for amide-CO, and intense band in the range of 1378–1351 and 1028–976 cm^{-1} assigned to strongly coupled between C=S and C–N vibrations. The ^{1}H NMR spectrum of **4a** (in $CDCl_3$) as an example showed sharp singlet at $\delta_H = 3.62$ ppm with integration equal to four protons due to $(CH_2)_2$ group; three multiplets were appeared; one at $\delta_H = 4.12$, 4.01 with four protons for two allyl-CH_2N, and another two multiplets at δ_H 5.12–5.09 due to allyl-CH_2 = and at δ_H 5.86–5.91 for allyl-CH= , and finally doublet of doublet signals at $\delta_H = 4.75$ and 4.87 ppm with ($J = 3.62$ Hz) for diastereotopic benzyl-CH_2 group. The ^{13}C NMR spectra of compounds **4a–e** showed carbon signals at $\delta_C = 51.22$ and 53.16 ppm which was assigned to $(CH_2)_2$. Two carbon signals; one at $\delta_C = 56.63$ and other at $\delta_C = 56.66$ ppm assigned to CH_2Ph. Carbon signals were also appeared at $\delta_C = 90.17$ (chiral-C, C-4), 175.12 (amide C=O) and 181.12 ppm (cyclic C=S). For **4a**, mass spectroscopy revealed an ion peak at $m/z = 588$ represents the fragment formed by release of the corresponding two allyl groups from the molecular ion. Also, the structure of **4a–e** containing two asymmetric carbon atoms, so, more than one alternative stereoisomer can be expected. To prove the structure of compounds **4a–e** unambiguously, single

crystals of **4a** was obtained. The X-ray crystallographic analysis confirmed the molecular structure of compounds **4a**–**e** and presence of two stereogenic centers and the molecule is *meso*. The structure of (R) 3-allyl-1-(((S) 3-allyl-4-benzyl-5-oxo-4-phenyl-2-thioxoimidazolidin-1-yl) ethyl)-5-benzyl-5-phenyl-2-thioxo-imidazolidin-4-one (**4a**) was determined by X-ray analysis (Fig. 2, Table S1 in supplementary data). The imidazolidine rings have only a slightly non-planar conformation (mean deviation from the L.S.-plane N3-C4-N5-C6-C7 and N24-C25-N26-C27-C28 are 0.018 Å and 0.008 Å, respectively) and are twisted by 26° (angle between the two L.S.-planes).

Scheme 2 cites a possible reaction mechanism based on the condition of our reaction. Firstly, the formation of compounds **3a** and **3b** was described as due to the internal cyclization by the nucleophilic addition of the nitrogen lone pair of one thiourea to the electrophilic-C of the C=S in the second thiourea group. The latter process accompanied with extrusion of one molecule of amine. Secondly, formation of compounds **4a**–**e** was explained as due to the addition of **1a**–**e** on the carbonyl group in **2** to form intermediate Zwitter-ion **6**. Subsequently, nucleophilic addition of thioamide-NH to conjugated C=C afforded the formation of intermediate **7,** which would be neutralized into **8**. On repeating the previous steps of the reaction with the second thiourea group in **1a**–**c** with another molecule of **2**, intermediates **9** to **11** would be formed and consequently compounds **4a**–**e** would be obtained (Scheme 2).

Biology

Cell Viability assay

The human mammary gland epithelial (MCF-10A) cell line was used to test the viability of novel compounds **4a**–**e** [24, 25]. MCF-10A cells were treated for four days with **4a**–**e** before being tested for viability using the MTT assay. According to Table 1, none of the compounds tested were cytotoxic, and cell viability was greater than 87% for the compounds tested at 50 µM.

Antiproliferative assay

Compounds **4a**–**e** were tested for antiproliferative activity against four human cancer cell lines using the MTT assay [26–29] and doxorubicin as the reference drug: Panc-1 (pancreas cancer cell line), MCF-7 (breast cancer cell line), HT-29 (colon cancer cell line), and A-549 (epithelial cancer cell line). Table 1 displays the median inhibitory concentration (IC_{50}).

In general, the tested compounds **4a**–**e** demonstrated promising antiproliferative activity against the four cancer cell lines, with GI_{50} ranging from 1.20 µM to 4.00 µM in comparison to the reference doxorubicin (GI_{50} = 1.10). Compounds **4c**–**e**, n = 3, were more potent than compounds **4a** and **4b**, where the linker was only two carbon atoms (n = 2), indicating the importance of linker length in these compounds' antiproliferative effect. Compound **4c** (R = allyl, n = 3) was the most potent, with an average GI_{50} value of

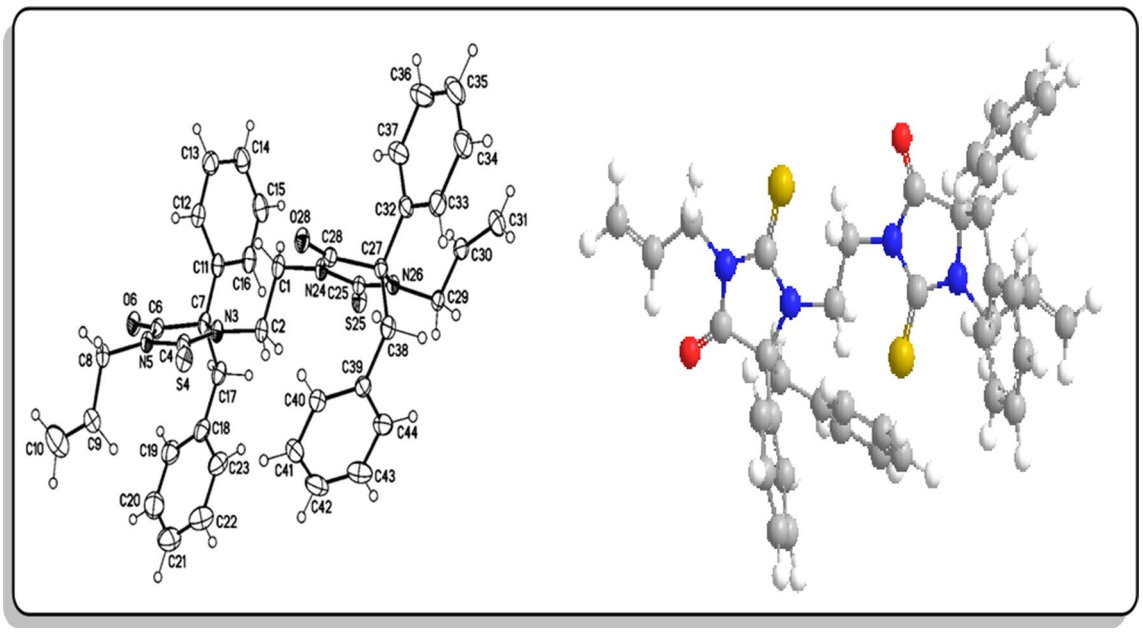

Fig. 2 X-ray structure analysis of (R) 3-allyl-1-(((S) 3-allyl-4-benzyl-5-oxo-4-phenyl-2-thioxoimidazolid-in-1-yl)ethyl)-5-benzyl-5-phenyl-2-thioxoimidazolidin-4-one (**4a**) (displacement parameters are drawn at 30% probability level)

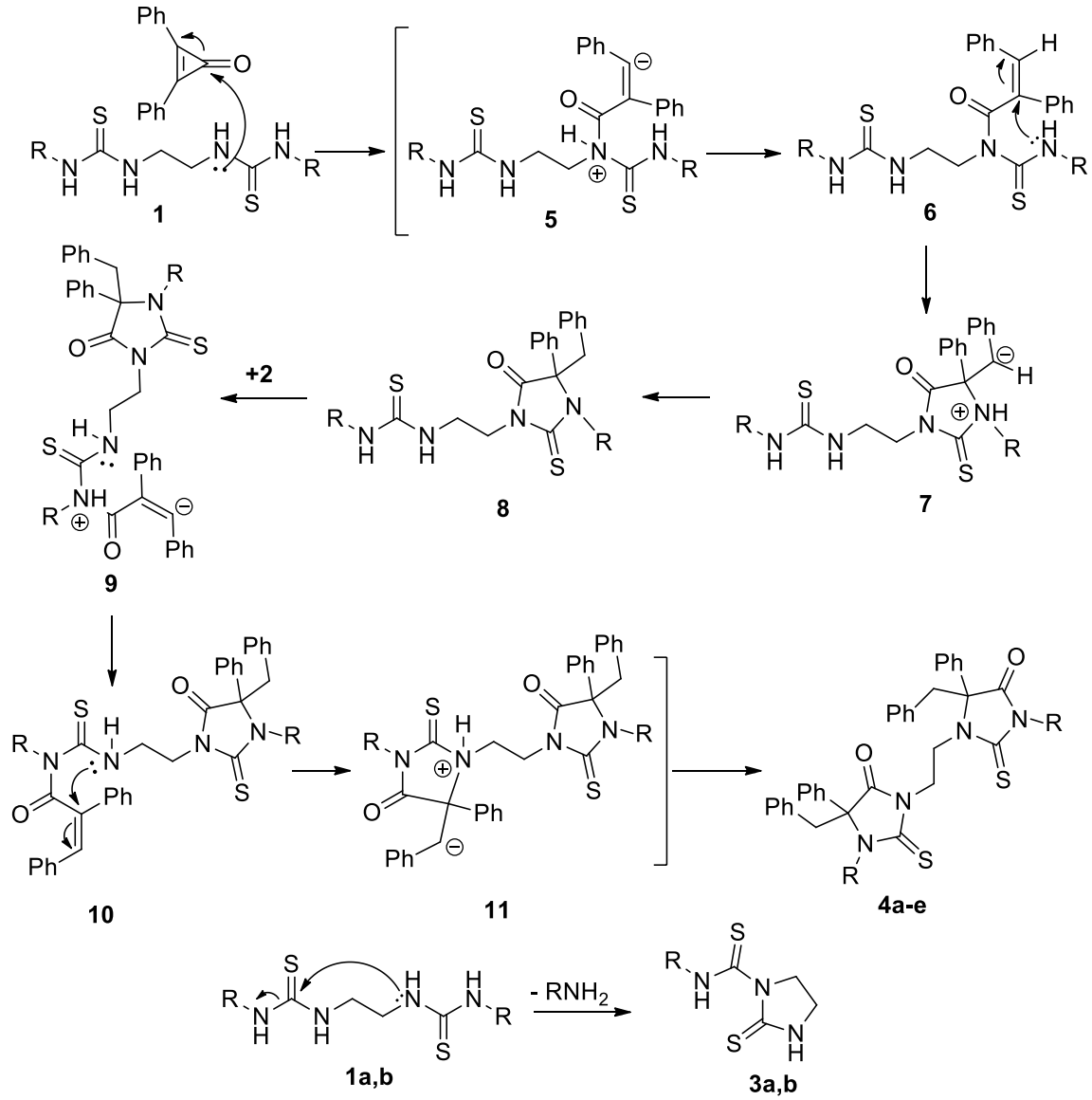

Scheme 2 The plausible mechanism for the formation of compounds **3a**, **3b**, and **4a–e**

1.20 µM, which was equivalent to the reference doxorubicin's GI_{50} value of 1.10 µM. In terms of activity against the four cancer cell lines, compound **4c** is almost as effective as doxorubicin. Replacement of the allyl group in compound **4c** with the phenyl group in compound **4e** (R = phenyl, n = 3) resulted in a slight decrease in antiproliferative activity of compound **4e**, with a GI_{50} of 1.50 µM compared to 1.20 µM for **4c**. Furthermore, replacing the allyl group in **4c** with ethyl group in **4d** (R = ethyl, n = 3) resulted in a significant decrease in antiproliferative effect, with compound **4d** GI_{50} equal to 1.70 µM being 1.4-fold less potent than **4c**. These results illuminated the significance of the substitution pattern at the imidazolidine moiety's position 3, where allyl group exhibit the highest activity, followed by phenyl group, and ethyl group exhibit the lowest action. Finally, compounds **4a** (R = allyl, n = 2) and **4b** (R = phenyl, n = 2) had lowest activity with GI_{50} values of 4.00 µM and 2.40 µM, respectively being 3-folds and 1.5-folds less potent than **4c** (R = allyl, n = 3) and **4e** (R = phenyl, n = 3), respectively.

EGFR inhibitory assay

The EGFR-TK assay [30, 31] was used to evaluate the EGFR inhibitory potency of compounds **4b–e**; the results are displayed in Table 2. The tested compounds showed EGFR inhibitory activity with IC_{50} values ranging from 90 to 178 nM in comparison to the reference erlotinib which had an IC_{50} value of 70 nM. The tested compounds in every instance were less effective than erlotinib. The outcomes of this test were consistent with those of a cancer cell-based

Table 1 IC_{50} of compounds **4a-e** and Doxorubicin

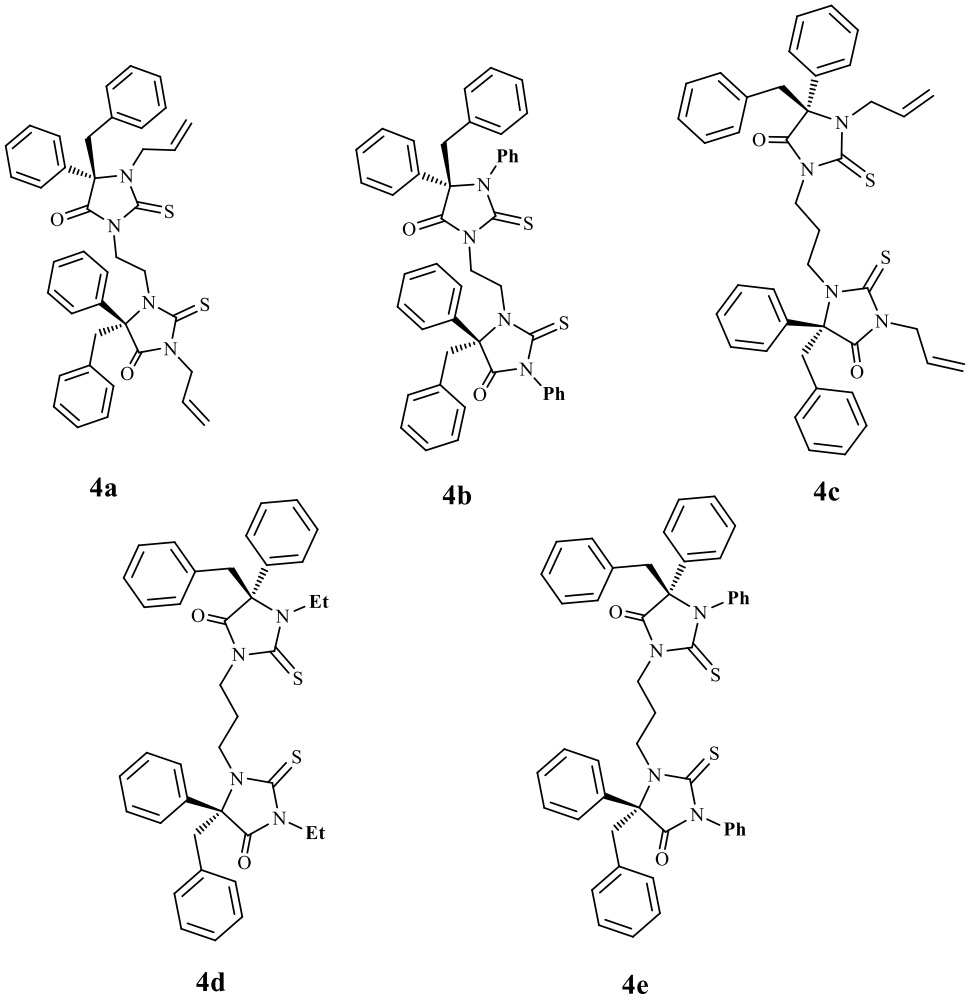

Compd	Cell viability %	Antiproliferative activity $IC_{50} \pm SEM$ (nM)				
		A-549	MCF-7	Panc-1	HT-29	Average
4a	89	3.90 ± 0.30	3.70 ± 0.30	4.20 ± 0.30	4.20 ± 0.30	4.00
4b	86	2.40 ± 0.20	2.10 ± 0.20	2.60 ± 0.20	2.60 ± 0.20	2.40
4c	91	1.30 ± 0.10	1.00 ± 0.10	1.40 ± 0.10	1.20 ± 0.10	1.20
4d	90	1.60 ± 0.10	1.50 ± 0.10	1.80 ± 0.10	1.80 ± 0.10	1.70
4e	85	1.40 ± 0.10	1.20 ± 0.08	1.60 ± 0.10	1.60 ± 0.10	1.50
Doxorubicin	–	1.20 ± 0.10	0.90 ± 0.10	1.40 ± 0.10	1.00 ± 0.10	1.10

Table 2 IC_{50} of compounds **4b–e** and Erlotinib

Compound	EGFR $IC_{50} \pm SEM$ (nM)
4b	178 ± 12
4c	90 ± 7
4d	128 ± 10
4e	107 ± 8
Erlotinib	70 ± 5

assay, in which compound **4c** (R = allyl, n = 3), the most potent antiproliferative, had the highest inhibitory effect on EGFR with an IC_{50} value of 90 nM, as opposed to erlotinib's IC_{50} value of 70 nM. The second and third-most active compounds were **4e** (R = phenyl, n = 3) and **4d** (R = ethyl, n = 3) and with IC_{50} values of 107 nM and 128 nM. Finally, compound **4b** (R = phenyl, n = 2) was the least effective EGFR inhibitor, with an IC_{50} value of 178 nM. These findings

imply that the compounds tested had a significant antiproliferative effect as well as the ability to act as an EGFR inhibitor.

Molecular docking simulations

As discussed previously in results and discussion section, how effectiveness is the 2-thioxo-4-imidazolidin-4-ones as EGFR inhibitors, we decided to explore their possible interaction modes within the active sites of EGFR. Molecular docking simulations of compounds (4a–e) within EGFR active site revealed their good interaction profile as summarized in Table 3.

Visual inspections of binding interactions of best docking pose of each tested compound and the co-crystallized ligand (Erlotinib), showed stabilization of their molecules inside cavity of active site with number of H-bonds and pi-H hydrophobic interactions with various amino acid residues lining active site, as shown in Figs. 3 and 4. Compound **4c** showed the highest docking score (S = − 6.88 kcal/mol) among the five tested compounds better than the reference; Erlotinib (S = − 6.88 kcal/mol). Additionally, Compound **4c** has two hydrogen bonds with Ser 696 and Phe 699 whereas Erlotinib form one hydrogen bond with Ser 696.

Conclusion

In conclusion, we have successfully developed a new strategy for the preparation of (2-(3-substituted-4-benzyl-5-oxo-4-phenyl-2-thioxoimidazolidin-1-yl)ethyl)-5-benzyl-5-phenyl-2-thi-oxoimidazolidin-4-ones through nucleophilic addition of N,N″-(1,ω-alkanediyl)bis(N′-organyl thiourea) derivatives and ring opening of 2,3-diphenylcyclopropanone. One the basis of the expected biological activity of the formed imidazole thione moiety the antiproliferative activity of the obtained products was also investigated. In comparison to erlotinib, which served as a control and had an IC_{50} value of 70 nM, the compounds tested showed EGFR inhibitory activity with IC_{50} values ranging from 90 to 178 nM. The most effective antiproliferative agent was discovered to be compound **4c**. When compared to erlotinib, which has an IC_{50} value of 70 nM, it had the most potent inhibitory effect on EGFR, with an IC_{50} value of 90 nM. Compounds **4e** and **4d** were the second and third most active compounds, with IC_{50} values of 107 nM and 128 nM, respectively. The compounds studied were both EGFR inhibitors and had a significant antiproliferative effect, according to the findings. The new compounds reported here are currently undergoing structural modifications in order to synthesize a new series of compounds that will be subjected to additional in vitro and in vivo assays in the hopes of obtaining a lead compound for drug design.

Experimental

Chemistry

General details

See Appendix A (Supplementary File)

N,*N*″-(1,*ω*-Alkanediyl)bis(*N*′-organyl thiourea) derivatives **1a**–**e** were prepared according to literature methods [17, 18]

Syntheses of imidazolidinethione and bis imidazolidinethione derivatives (3a, 3b, and 4a-e)

General procedure

A solution of **1a**–**e** (1.0 mmol) in absolute ethanol (20 ml), a solution of **2** (1.0 mmol) in absolute ethanol (20 ml) was added dropwise with stirring. The mixture was stirred for 30 min, then the mixture was refluxed for 6–8 h (the reaction was monitored by TLC analyses). The reaction mixture was concentrated, and the residue was subjected to chromatographic plates using toluene-ethyl acetate (5:2) as

Table 3 Binding Interactions of **4a**–**e** and Erlotinib within EGFR (PDB ID: 1M17) active sites

	4a	4b	4c	4d	4e	Erlotinib
	EGFR (PDB ID): 1M17					
S (kcal/mol)	− 6.44	− 6.56	− 6.88	− 6.78	− 6.82	− 6.27
RMSD (Å)	1.75	1.76	1.93	1.64	1.42	1.46
Amino acids residues binding interactions & their bond length (Å)	Lys 721 (3.96)[a]	Gly 772 (4.00)[a]	Ser 696 (3.99)[a] Phe 699(3.86)[b]	Gly 695 (3.95)[c] Phe 699 (4.12)[b]	Lys 721 (3.98) Phe 699 (3.93)[b] Leu 694 (4.21)[b]	Ser 696 (3.46)[a]

[a]H-acceptor

[b]pi-H

[c]H-donor

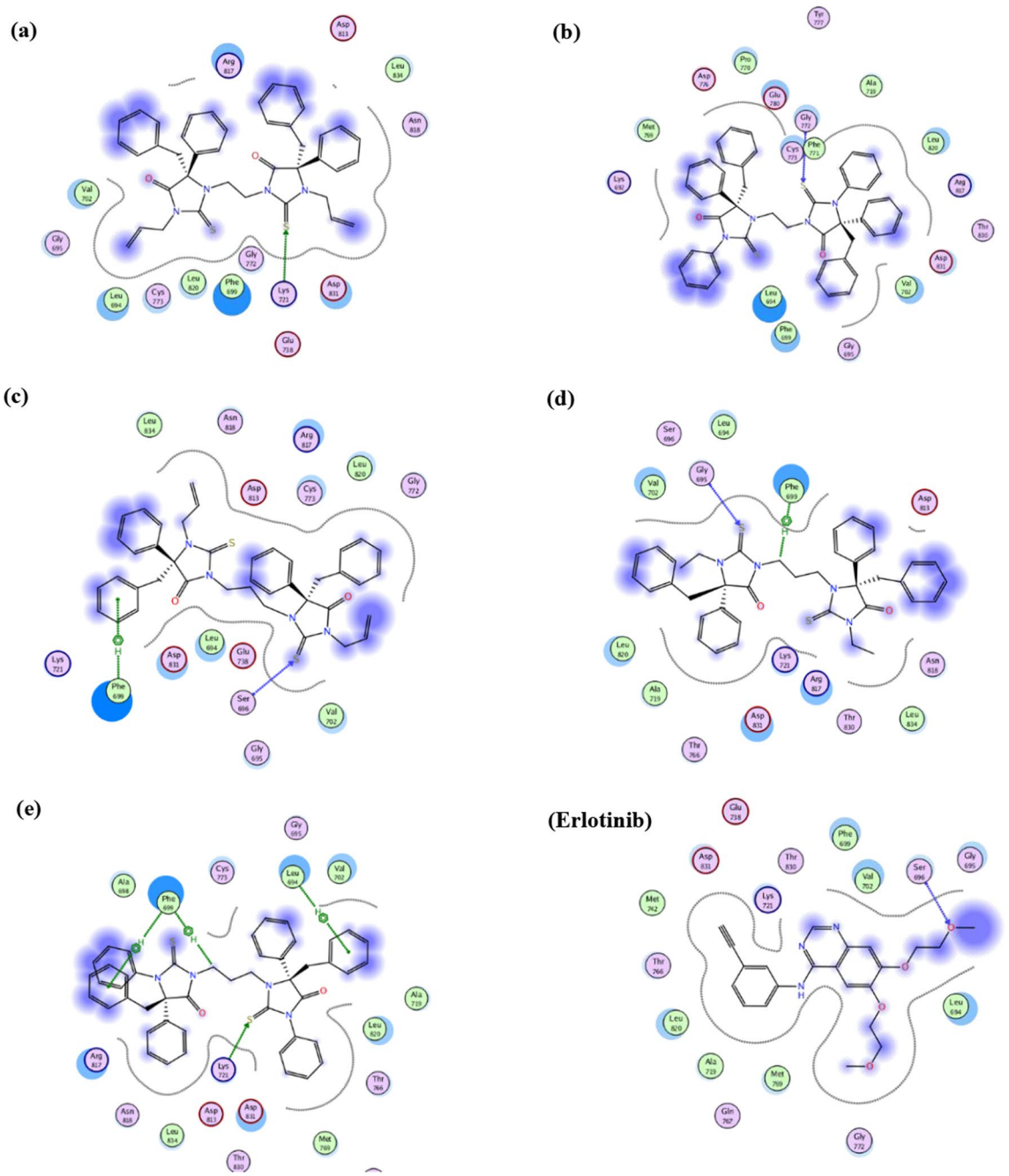

Fig. 3. 2D Interaction diagram of **4a**–**e**and **Erlotinib** within EGFR (PDB ID: 1M17) active site showing H-bonding (green and blue arrows), pi-H (green dotted-line), and proximity contour around each molecule (grey dotted-line)

eluent. The fastest migration zone contains the imidazolidine thione derivatives **3a,b** (4–6%), the slowest migrating zone containing bis-imidazolidine thione derivatives **4a**–**e** (68–60%), the products obtained were recrystallized from the stated solvents.

N-Allyl-2-thioxoimidazolidine-1-carbothioamide (**3a**). 4%, mp 123–125 (lit. 126–128) °C [27].

N-Phenyl-2-thioximidazolidine-1-carbothioamide (**3b**). 6%, mp 176–177 (lit. 176–177) °C [28].

(R) 3-allyl-1-(((S) 3-allyl-4-benzyl-5-oxo-4-phenyl-2-thioxoimidazolidin-1-yl)ethyl)-5-benzyl-5-phenyl-2-thioxoimidazolidin-4-one (4a) Colorless crystals (EtOH); m.p 268–270 °C; yield:456.2 mg (68%); IR: 3090–3081 (Ar–CH),

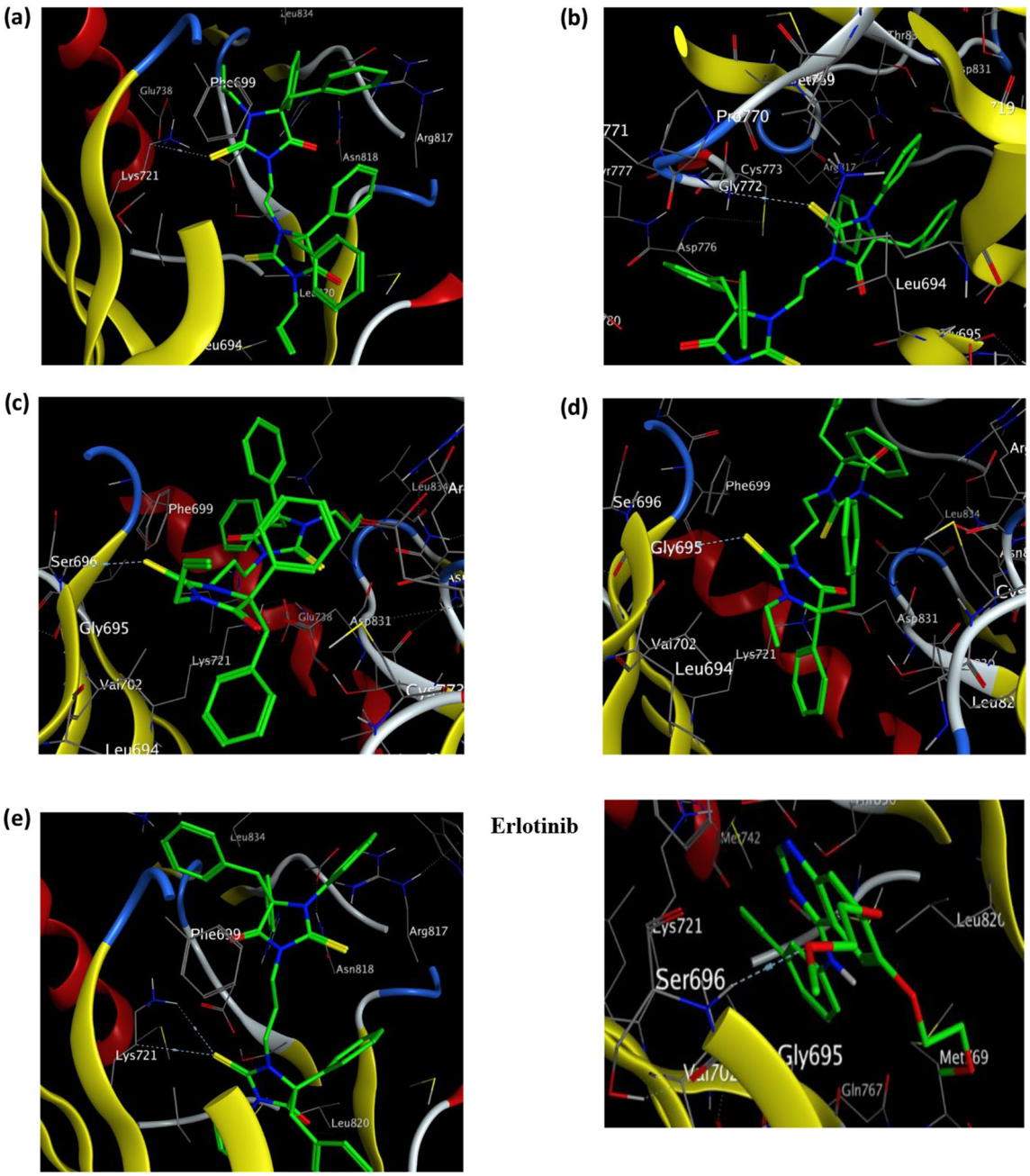

Fig. 4. 3D Interaction diagram of 4a–e & Erlotinib within EGFR (PDB ID: 1M17)

2966 (ali-CH_2) 1686 (C=O), 1361 cm^{-1} (C=S and C–N); ^{1}H NMR ($CDCl_3$): δ_H = 3.37–3.62 (m, 4H, –CH_2), 4.02–4.12 (m, 4H, allyl-CH_2N), 4.75–4.77 (d, J = 3.62 Hz, 4H, benzyl-CH_2), 5.09–5.12 (m, 4H, allyl-CH_2=), 5.86–5.91 (m, 2H, allyl-CH=), 7.03–7.11 (m, 8H, Ar–H), 7.21–7.28 (m, 8H, Ar–H), 7.38–7.41, 7.48, 7.53 ppm (m, 4H, Ar–H); ^{13}C NMR ($CDCl_3$): δ_C = 51.23, 53.16 (CH_2), 54.48 (allyl-CH_2), 56.63, 56.66 (benzyl-CH_2), 90.17 (***C***-5), 116.53 (allyl-CH_2=), 126.95, 127.12, 127.16,128.12, 128.0.39, 128.84, 129.12, 129.36 (Ar–CH), 131.12, 132.44, 133.71 (Ar–C), 135.45 (allyl-CH=), 175.12 (C=O), 181.12 ppm (C=S). MS (70 eV, %): *m/z* = 670 (M^+, 41), 588 (18), 335 (87), 92 (100), 41 (76). *Anal. Calcd. For* $C_{40}H_{38}N_4O_2S_2$ (670.89): C, 71.61; H, 5.71; N, 8.35; S, 9.56. Found: C, 71.73; H, 5.80; N, 8,41; S, 9.59.

(S)-5-benzyl-3-(2-((R)-5-benzyl-4-oxo-3,5-diphenyl-2-thioxoimidazolidin-1-yl)ethyl)-1,5-diphenyl-2-thioxoimidazolidin-4-one (4b) Colorless crystals (CH_3CN); m.p 260–262 °C; yield 482.9 mg (65%); IR: 3100–3085 (Ar–CH),

2954–2942 (ali-CH_2) 1684 (C=O), 1358 cm^{-1} (C=S and C–N); ^{1}H NMR ($CDCl_3$): δ_H = 3.22 (m, 4H, –CH_2), 3.74–3.41 (d, 4H, benzyl-CH_2), 6.80–7.15 (m, 10H, Ar–H), 7.40–7.53 ppm (m, 20H, Ar–H); ^{13}C NMR ($CDCl_3$): δ_C = 45.98, 47.62 (benzyl-CH_2), 53.22 (CH_2), 92.17 (***C-5***), 126.12, 126.81, 127.69, 127.79, 128.11, 128.18, 128.25, 128.37, 128.52, 129.30, 129.39 (Ar–CH), 135.76, 138.03, 141.71, 142.84 (Ar–C), 173.64 (CO), 178.84 ppm (C=S). MS (70 eV, %): *m/z* = 742 (M^+, 67), 558 (46), 371 (100), 92 (82). *Anal. Calcd. For* $C_{46}H_{38}N_4O_2S_2$ (742.95): C, 74.36; H, 5.16; N, 7.54; S, 8.63. Found: C, 74.48; H, 5.22; N, 7.46; S, 8.58.

(R) 3-allyl-1-(((S) 3-allyl-4-benzyl-5-oxo-4-phenyl-2-thioxoimidazolidin-1-yl)propyl)-5-benzyl-5-phenyl-2-thioxoimidazolidin-4-one (4c) Colorless crystals (CH_3OH); m.p 243–245 °C; yield: 431.4 mg (63%); IR (KBr): υ = 3086–3078 (Ar–CH), 2978–2966 (ali-CH_2) 1681 (C=O), 1358 cm^{-1} (C=S and C–N); ^{1}H NMR ($CDCl_3$): δ_H = 1.76 (m, 2H, CH_2), 3.68 (t, 2H, CH_2), 4.21 (t, 2H, CH_2), 4.25–4.27 (m, 4H, allyl-CH_2N), 4.73, 4.85 (d, 4H, benzyl-CH_2), 5.11–514 (m, 4H, allyl-CH_2=), 5.89–5.92 (m, 2H, allyl-CH=), 7.09–7.11 (m, 8H, Ar–H), 7.31–7.56 ppm (m, 12H, Ar–H); ^{13}C NMR ($CDCl_3$) δ_C = 25.16 (CH_2), 49.62 (CH_2), 55.07 (allyl-CH_2), 50.06 (CH_2), 90.64 (***C***-5), 116.74 (allyl-CH_2=), 125.9, 126.6, 127.6, 127.7,128.6, 129.2, 129.6 (Ar–CH), 131.76, 132.64, 133.84 (Ar–C), 135.83 (allyl-CH=), 174.93 (C=O), 181.28 ppm (C=S). MS (70 eV, %): *m/z* = 684 (M^+, 54), 642 (28), 352 (37), 358(18), 92 (36), 42 (38). *Anal. Calcd. For* $C_{41}H_{40}N_4O_2S_2$ (684.91): C, 71.90; H, 5.89; N, 8.18; S, 9.36. Found: C,71.98; H, 5.94; N,8,09; S, 9.42.

(S)-5-benzyl-3-(3-((R)-5-benzyl-3-ethyl-4-oxo-5-phenyl-2-thioxoimidazolidin-1-yl)propyl)-1-ethyl-5-phenyl-2-thioxoimidazolidin-4-one (4d) Colorless crystals (CH_3CN); m.p 254–256 °C; yield: 436.18 mg (66%); IR: 3072–3064 (Ar–CH), 2984–2964 (ali-CH_2) 1684 (C=O), 1364 cm^{-1} (C=S and C–N); ^{1}H NMR ($CDCl_3$): δ = 1.28 (t, *J* = 7.01, 6H, 2CH_3), 1.69 (m, 2H, CH_2), 3.06, 3.38 (d, 2H, benzyl-CH_2), 3.42 (t, 2H, -CH_2), 3.51 (q, *J* = 7.01 Hz; 2H, ethyl-CH_2), 4.08 (q, *J* = 7.01 Hz; 2H, ethyl-CH_2), 4.12 (t, 2H, CH_2), 6.96–7.27 (m, 10 H, Ar–H), 7.28–7.54 ppm (m, 10H, Ar–CH); ^{13}C NMR ($CDCl_3$) δ_C = 12.64 (CH_3), 13.37 (CH_3), 24.71 (CH_2), 45.76 (CH_2-ethyl), 46.63 (CH_2-ethyl), 47.93, 49.62 (benzyl-CH_2), 126.32, 126.81, 127.76, 127.71, 128.80, 129.22, 129.63 (Ar–C), 135.53, 139.46, 141.12, (Ar–C), 177.41 (C=O), 178.55 ppm (C=S). MS (70 eV, %): *m/z* = 660 (M^+, 74), 631 (22), 602 (19), 337 (31), 309 (21), 92 (64), 29 (33). *Anal. Calcd. For* $C_{39}H_{40}N_4O_2S_2$ (660.84): C, 70.88; H, 6.10; N, 8.48; S, 9.70. Found C,70.76; H, 6.14; N,8.53; S, 9.67.

(S)-5-benzyl-3-(3-((R)-5-benzyl-4-oxo-3,5-diphenyl-2-thioxoimidazolidin-1-yl)propyl)-1,5-diphenyl-2-thioxoimidazolidin-4-one (4e) Colorless crystals (CH_3CN), m. p. 242–244 °C; yield 454.18 mg (60%); IR (KBr): υ = 3068–3063 (Ar–CH), 2988–2976 (ali-CH_2) 1677 (C=O), 1358 cm^{-1} (C=S and C–N); ^{1}H NMR ($CDCl_3$): δ_H = 1.71–1.74 (m, 2H, CH_2), 3.11, 3.46 (d, 4H, benzyl-CH_2), 3.48 (m, 2H, -CH_2), 4.11 (m, 2H, CH_2), 6.65–6.80 (m, 4H, Ar–H), 7.21–7.25 (m, 9H Ar–CH), 7.27–7.29 (m, 9H, Ar–CH), 7.40–7.43 ppm (m, 8H, Ar–CH); ^{13}C NMR ($CDCl_3$) δ = 24.31 (CH_2), 47.91 (CH_2), 41.12, 40.48 (benzyl-CH_2), 90.63, 90.82 (***C-5,5′***), 139.26, 136.51, 141.42, 140.54, 140.94 (Ar–C), 177.41 (C=O), 178.55 ppm (C=S). MS (70 eV, %): *m/z* = 756.2 (M^+, 46), 572 (38), 371 (26), 399 (29), 92 (61). *Anal. Calcd. For* $C_{47}H_{40}N_4O_2S_2$ (756.2): C, 74.57; H, 5.33; N, 7.40; S, 8.47. Found: C,74.61; H, 5.28; N,7.46; S, 8.41.

Crystal structure determinations of 3b and 4a

The single-crystal X-ray diffraction studies were carried out on a Bruker D8 Venture diffractometer with Photon II detector at 173(2) K using Cu-Kα radiation (λ = 1.54178 Å). Dual space methods (SHELXT for **5a**) [G. M. Sheldrick, *Acta Crystallogr.* 2015, **A71**, 3–8] were used for structure solution and refinement was carried out using SHELXL-2014 (full-matrix least-squares on F^2) [G. M. Sheldrick, *Acta Crystallogr.* 2015, **C71**, 3–8]. Hydrogen atoms were refined using a riding model. Semi-empirical absorption corrections were applied.

3b: colourless crystals, $C_{10}H_{11}N_3S_2$, M_r = 237.34, crystal size 0.20 × 0.12 × 0.04 mm, monoclinic, space group $P2_1/c$ (No. 14), *a* = 7.4431(5) Å, *b* = 12.1308(8) Å, *c* = 12.2679(8) Å, β = 103.162(3)°, *V* = 1078.58(12) $Å^3$, *Z* = 4, ρ = 1.462 Mg/m^{-3}, μ(Cu-K_α) = 4.22 mm^{-1}, *F*(000) = 496, *T* = 173 K, $2\theta_{max}$ = 144.6°, 10057 reflections, of which 2125 were independent (R_{int} = 0.035), 196 parameters, 615 restraints (see cif-file for details), R_1 = 0.047 (for 2034 I > 2σ(I)), wR_2 = 0.127 (all data), *S* = 1.09, largest diff. peak/hole = 0.59/− 0.30 e $Å^{-3}$. Disorder of the complete molecule (about a twofold axis), 90:10 (determined at the stage of the isotropic refinement and then fixed), minor disordered part refined isotropically (see cif-file for details).

4a: colourless crystals, $C_{40}H_{38}N_4O_2S_2$, M_r = 670.86, crystal size 0.21 × 0.18 × 0.03 mm, monoclinic, space group $P2_1/n$ (No. 14), *a* = 11.7727(3) Å, *b* = 13.6117(3) Å, *c* = 22.3014(5) Å, β = 92.596(1)°, *V* = 3570.05(14) $Å^3$, *Z* = 4, ρ = 1.248 Mg/m^{-3}, μ(Cu-K_α) = 1.67 mm^{-1}, *F*(000) = 1416, *T* = 173 K, $2\theta_{max}$ = 144.8°, 37307 reflections, of which 7054 were independent (R_{int} = 0.029), 433 parameters, 387 restraints (see cif-file for details) R_1 = 0.057 [for 6383 I > 2σ(I)], wR_2 = 0.160 (all data), *S* = 1.04, largest diff. peak/hole = 0.78/− 0.28 e $Å^{-3}$.

CCDC 2235115 (**3b**), and 2235116 (**4a**) contain the supplementary crystallographic data for this paper. These data can be obtained free of charge from The Cambridge Crystallographic Data Centre via www.ccdc.cam.ac.uk/data_request/cif.

Protocol of docking studies

The automated docking simulation study is performed using Molecular Operating Environment (MOE®) version 2014.09. The X-ray crystallographic structure of the target EGFR obtained from the protein data bank (PDB: 1M17), was obtained from Protein data bank. The target compounds were constructed into a 3D model using the builder interface of the MOE® program. After checking their structures and the formal charges on atoms by 2D depiction, the following steps were carried out: The target compounds were subjected to a conformational search. All conformers were subjected to energy minimization; all the minimizations were performed with MOE until a RMSD gradient of 0.01 kcal/mole and RMS distance of 0.1 Å with MMFF94X force-field and the partial charges were automatically calculated. The protein was prepared for docking studies by adding hydrogen atoms to the system with their standard geometry. The atoms connection and type were checked for any errors with automatic correction. Selection of the receptor and its atoms potential were fixed. MOE Alpha Site Finder was used for the active site search in the enzyme structure using all default items. Dummy atoms were created from the obtained alpha spheres.

Acknowledgements We gratefully acknowledge the support of the Karlsruhe Institute of Technology's KIT-Publication Fund. The National Science Foundation of the United States aided in the purchase of the NMR spectrometer at Florida Institute of Technology (CHE 03 42251).

Author contributions Alaa A. Hassan, A.A. Aly, Mohamed Ramadan, and Bahaa G. M. Youssif :Conceptualization, writing, and editing and revision, Nasr K. Mohamed, B.G.M. Youssif and H.A.M. Gomaa: Biology, methodology, writing, and editing, S. Bräse and Martin Nieger: X-ray, editing. Amal S. Abd El-Aal: Methodology, writing. All authors reviewed the manuscript.

Funding No Funds.

Declarations

Competing interests The authors declare no competing interests.

Conflict of interest The authors declare no conflict of interest.

References

1. Saravani F, Moghadam ES, Salehabadi H, Ostad S, Hamedani MP, Amanlou M, Faramarzi MA, Amini M (2019) Synthesis, anti-proliferative evaluation, and molecular docking studies of 3-(alkylthio)-5,6-diaryl-1,2,4-triazines as tubulin polymerization inhibitors. Lett Drug Des Discov 16:1194–1201
2. Ashourpour M, Hosseini FM, Amini M, Moghadam ES, Kazerouni S, Arman SY, Shahsavari Z (2021) Pyrazole derivatives induce apoptosis via ROS generation in the triple negative breast cancer cells, MDA-MB-468. Asian Pac J Cancer Prev 22(7):2079–2087
3. Arafeh MM, Moghadam ES, Adham SAI, Stoll R, Abdel-Jalil RJ (2021) Synthesis and cytotoxic activity study of novel 2-(aryldiazenyl)-3-methyl-1H-benzo[g]indole derivatives. Molecules 26:4240
4. Attiq A, Jalil J, Husain K, Ahmad W (2018) Raging the war against inflammation with natural products. Front Pharmacol 9:976–1002
5. Muccioli GG, Fazio N, Scriba GKE, Poppitz W, Cannata F, Poupaert JH, Wouters J, Lambert DM (2006) Substituted 2-thioxoimidazolidin-4-ones and imidazolidine-2,4-diones as fatty acid amide hydrolase inhibitors templates. J Med Chem 49:417–425
6. Kim HR, Lee HJ, Choi P, Park YJ, Woo Y, Kim SJ, Park MH, Lee HW, Chun P, Chung HY, Moon HR (2014) Benzylidene linked thiohydantoin derivatives as inhibitors of tyrosinase and melanogenesis: importance of the β-phenyl-α,β-unsaturated carbonyl functionality. Med Chem Commun 5:1410–1417
7. Orwat W, Korona-Głowniak B, Barbasz I, Kownacki A, Latacz I, Handzlik G, Zesławska J, Malm E (2019) Highly efficient microwave synthesis of rhodanine and 2-thiohydantoin derivatives and determination of relationships between their chemical structures and antibacterial activity. RSC Adv 9:39367–39380
8. Camargo PG, da Silva Bortoleti BT, Fabris M, Gonçalves MD, Tomiotto-Pellissier F, Costa IN, Conchon-Costa I, da Silva Lima CH, Pavanelli WR, de Lima Ferreira Bispo M, Macedo F Jr (2022) Thiohydantoins as anti-leishmanial agents: in vitro biological evaluation and multi-target investigation by molecular docking studies. J Biomol Struct Dyn 40:3213–3222
9. Wu F, Jiang H, Zheng B, Kogiso M, Yao Y, Zhou C, Li X-N, Song Y (2015) Inhibition of cancer-associated mutant isocitrate dehydrogenases by 2-thiohydantoin compounds. J Med Chem 58:6899–6908
10. Cho S, Kim S-H, Shin D (2019) Recent applications of hydantoin and thiohydantoin in medicinal chemistry. Eur J Med Chem 164:517–545
11. Tran C, Ouk S, Clegg NJ, Chen Y, Watson PA, Arora V, Wongvipat J, Smith-Jones PM, Yoo D, Kwon A et al (2009) Development of a second-generation antiandrogen for treatment of advanced prostate cancer. Science 324:787–790
12. Lee TH, Khan Z, Kim SY, Lee KR (2019) Thiohydantoin and hydantoin derivatives from the roots of armoracia rusticana and their neurotrophic and anti-neuro inflammatory activities. J Nat Prod 82:3020–3024
13. Haslak ZP, Cinar SA, Ozbek SS, Monard G, Dogan I, Aviyente V (2020) Elucidation of the Z. P. atroposelectivity in the synthesis of axially chiral thiohydantoin derivatives. Org Biomol Chem 18:2233–2241
14. Králová P, Maloˇn M, Koshino H, Soural M (2018) Convenient synthesis of thiohydantoins, imidazole-2-thiones and imidazo[2,1-b]thiazol-4-Iums from polymer-supported β-acylamino ketones. Molecules 23:976–983
15. Wang ZD, Sheikh SO, Zhang YA (2006) Simple synthesis of 2-thiohydantoins. Molecules 11:739–750

16. Majumdar P, Bathula C, Basu SM, Das SK, Agarwal R, Hati S, Singh A, Sen S, Das BB (2015) Design, synthesis, and evaluation of thiohydantoin derivatives as potent topoisomerase i (top1) inhibitors with anticancer activity. Eur J Med Chem 102:540–551
17. Azizmohammadi M, Khoobi M, Ramazani A, Emami S, Zarrin A, Firuzi O, Miri R, Shafiee A (2003) 2H-chromene derivatives bearing thiazolidine-2,4-dione, rhodanine or hydantoin moieties as potential anticancer agents. Eur J Med Chem 59:15–22
18. Alanazi AM, El-Azab AS, Al-Swaidan IA, Maarouf AR, El-Bendary ER, Abu El-Enin MA, Abdel-Aziz AAM (2013) Synthesis, single-crystal, in vitro antitumor evaluation, and molecular docking of 3-substitued 5,5-diphenylimidazolidine-2,4-dione derivatives. Med Chem Res 22:6129–6142
19. Bae YS, Choi S, Park JJ, Cui M, Cho H, Lee WJ, Lee SH (2016) Synthesis, and biological evaluation of 3-substituted 5-benzylidene-1-methyl-2-thiohydantoins as potent NADPH oxidase (NOX) inhibitors. Bioorg Med Chem 24:4144–4151
20. Yabuuchi T, HisAki M, Matuda M, Kimura R (1975) Synthesis of alkylenebis (thiourea) derivatives and their related compounds. Chem Pharm Bull 23:663–668
21. Hassan AA, Döpp D (2006) Thermolysis of N, N″-1, ω-alkanediyl-bis[n′-organylthiourea] derivatives. J Heterocyclic Chem 43:593–598
22. Hassan AA, Mourad AE, El-Shaieb KMA, AbouZied AH, Döpp D (2003) Thermolysis of symmetrical dithiobiurea and thioureidoethylthiourea derivatives. Heteroatom Chem 14:535–541
23. Matsumura N, Kusamiya M, Inoue H, Iwasaki F (1995) Synthesis and reactivities of 10-*S*-3 trithiadiazapentalene derivatives. J Heterocyclic Chem 32:1269–1275
24. Ramadan M, Abd El-Aziz M, Elshaier YAMM, Youssif BGM, Brown AB, Fathy HM, Aly AA (2020) Design and synthesis of new pyranoquinolinone heteroannulated to triazolopyrimidine of potential apoptotic antiproliferative activity. Bioorg Chem 105:104392
25. Mekheimer RA, Allam SMR, Al-Sheikh MA, Moustafa MS, Al-Mousawi SM, Mostafa YA, Youssif BGM, Gomaa HAM, Hayallah AM, Abdelaziz M, Sadek KU (2022) Discovery of new pyrimido[5,4-c]quinolines as potential antiproliferative agents with multitarget actions: rapid synthesis, docking, and ADME studies. Bioorg Chem 121:105693
26. Gomaa HAM, Shaker ME, Alzarea SI, Hendawy OM, Mohamed FAM, Gouda AM, Ali AT, Morcoss MM, Abdelrahman MH, Trembleau L, Youssif BGM (2022) Optimization and SAR investigation of novel 2,3-dihydropyrazino[1,2-a]indole-1,4-dione derivatives as EGFR and $BRAF^{V600E}$ dual inhibitors with potent antiproliferative and antioxidant activities. Bioorg Chem 120:105616
27. Al-Wahaibi LH, Gouda AM, Abou-Ghadir O, Salem OIA, Ali AT, Farghaly HS, Abdelrahman MH, Trembleau L, Abdu-Allah HHM, Youssif BGM (2020) Design and synthesis of novel 2,3-dihydropyrazino[1,2-a]indole-1,4-dione derivatives as antiproliferative EGFR and $BRAF^{V600E}$ dual inhibitors. Bioorg Chem 104:104260
28. AlA M, Abdel-Aziz SA, Abdelrahman KS, Wanas AS, Gouda AM, Youssif BGM, Abdel-Aziz M (2020) Design and synthesis of new 1,6-dihydropyrimidin-2-thio derivatives targeting VEGFR-2: molecular docking and antiproliferative evaluation. Bioorg Chem 102:104090
29. Gomaa HAM, El-Sherief HAM, Hussein S, Gouda AM, Salem OIA, Alharbi KS, Hayallah AM, Youssif BGM (2020) Novel 1,2,4.-triazole derivatives as apoptotic inducers targeting p53: synthesis and antiproliferative activity. Bioorg Chem 105:104369
30. Mohamed FAM, Gomaa HAM, Hendawy OM, Ali AT, Farghaly HS, Gouda AM, Abdelazeem AH, Abdelrahman MH, Trembleau L, Youssif BGM (2021) Design, synthesis, and biological evaluation of novel EGFR inhibitors containing 5-chloro-3-hydroxymethyl-indole-2-carboxamide scaffold with apoptotic antiproliferative activity. Bioorg Chem 112:104960
31. Abdel-Aziz SA, TaherLan P, Asaad GF, Gomaa HAM, El-Koussi NA, Youssif BGM, ES (2021) Design, synthesis, and biological evaluation of new pyrimidine-5-carbonitrile derivatives bearing 1,3-thiazole moiety as novel anti-inflammatory EGFR inhibitors with cardiac safety profile. Bioorg Chem 111:104890